Journal of Engineering Physics and Thermophysics, Vol. 81, No. 1, 2008

CONJUGATE PROBLEM OF THERMOGRAVITATIONAL CONVECTION IN A RECTANGULAR REGION WITH A LOCAL HEAT SOURCE

G. V. Kuznetsov[a] **and M. A. Sheremet**[b] UDC 669.86:536.21

Mathematical simulation of conjugate convective-conductive heat transfer in a closed rectangular region in the presence of a heat-release source is carried out. The distributions of the thermal and hydrodynamic parameters that characterize the basic laws of the process investigated have been obtained. The possibilities of a more detailed description of both the temperature fields of the system as a whole and of maximum temperatures using a plane conjugate model of convective-conductive heat transfer are shown.

Introduction. Simulation of conjugate heat transfer in the presence of local sources of heat release as well as under the conditions of nonlinear effect of the environment is of both fundamental and applied importance. A direct proof of this fact is the problem of the thermal state of typical electroradioelements (ERE). At the present time there is a trend toward miniaturization of the specimens of radioelectronic equipment (REE) and electronics (E) due to the necessity of improving the characteristics of radioelectronic and electronic systems. But the reduction of the overall dimensions and mass of REE and E also leads to an overall increase in the energy scattered per unit area [1]. At the same time, an analysis of the temperature fields of contemporary specimens of REE and E is carried out mainly using either simple balance models or models of heat transfer in which boundary conditions of the third kind are taken to describe the processes of heat exchange with the surrounding medium or with a cooling gas [2]. But the determination of the heat transfer coefficients for the existing diversity of working conditions, dimensions, configurations, and mutual arrangement of individual ERE is virtually impossible. Therefore, to carry out a more detailed analysis of the processes of heat transfer in electroradioelements it is necessary to use two- or three-dimensional models of convection and heat conduction. Here, an important feature of the problems considered is the conjugate character of heat transfer [3, 4].

The purpose of the present investigation was to simulate mathematically nonstationary conjugate convective-conductive heat transfer in a closed rectangular region with a local source of heat release under the conditions of convective-radiative heat exchange with the environment. The given problem is based on the extension of the model of [5, 6] to the regions corresponding to the conditions of operation of REE and E.

Mathematical Model. We considered a boundary-value problem of nonstationary conjugate heat transfer for the geometry presented in Fig. 1.

The object investigated consists of five rectangles having different dimensions and different thermophysical characteristics. The temperature on the heat release source remains constant during the entire process. The horizontal walls ($y = 0$, $y = L_y$) and the vertical wall ($x = L_x$) that form the gas cavity are assumed to be thermally insulated on the outside. On the outer boundary $x = 0$ there is convective-radiative heat exchange with the surrounding medium.

It is assumed that the thermophysical properties of the elements of the solid material and gas are independent of temperature and that the regime of flow is laminar. The gas is considered to be a Newtonian fluid, incompressible and satisfying the Boussinesq approximation. The motion of the gas and heat transfer in the inner volume are assumed to be plane, and radiative heat transfer from the source of heat release and between the walls to be negligibly small in comparison with convective heat transfer; the gas is considered to be perfectly transparent for thermal radiation.

The formulation given is a modification of the classical problem of the Rayleigh–Benard natural convection [7] in which the influence of the dynamics of conductive heat transfer in rather large elements with a high heat capacity of their materials on the outer contour of the gas cavity is also taken into account. The process of heat transfer

[a]Tomsk Polytechnic University, 30 Lenin Ave., Tomsk, 634050, Russia; [b]Tomsk State University, 36 Lenin Ave., Tomsk, 634050, Russia; email: Michael-sher@yandex.ru. Translated from Inzhenerno-Fizicheskii Zhurnal, Vol. 81, No. 1, pp. 90–96, January–February, 2008. Original article submitted September 12, 2006.

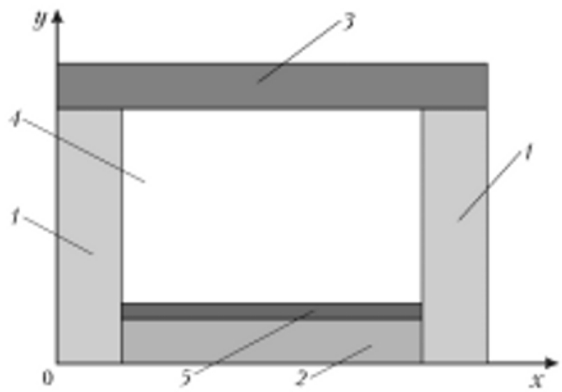

Fig. 1. Solution domain of the problem considered: 1–3) elements of the solid material; 4) gas cavity; 5) source of heat release.

in the region considered (Fig. 1) is described by a system of nonstationary two-dimensional equations of convection in the Boussinesq approximation in a gas cavity [8–10] and by a nonstationary two-dimensional equation of heat condition for the elements of the solid material [11] with nonlinear boundary conditions. The mathematical model is formulated in the dimensionless "stream function–vorticity–temperature" variables. As the scale of the distance, the length of the gas cavity over the x axis was selected. To make the system of equations nondimensional, the following relations were selected:

$$X = \frac{x}{L}\,, \quad Y = \frac{y}{L}\,, \quad \tau = \frac{t}{t_0}\,, \quad U = \frac{u}{V_0}\,, \quad V = \frac{v}{V_0}\,, \quad \Theta = \frac{T - T_0}{T_{\text{h.s}} - T_0}\,, \quad \Psi = \frac{\psi}{\psi_0}\,, \quad \Omega = \frac{\omega}{\omega_0}\,.$$

The dimensionless Boussinesq equations in the stream function–vorticity–temperature variables for the problem considered have the form:

in the gas cavity (Fig. 1)

$$\frac{1}{\text{Ho}}\frac{\partial \Omega}{\partial \tau} + \frac{\partial \Psi}{\partial Y}\frac{\partial \Omega}{\partial X} - \frac{\partial \Psi}{\partial X}\frac{\partial \Omega}{\partial Y} = \frac{1}{\sqrt{\text{Gr}}}\Delta\Omega + \frac{1}{2}\frac{\partial \Theta}{\partial X}\,, \tag{1}$$

$$\Delta\Psi = -\,2\Omega\,, \tag{2}$$

$$\frac{1}{\text{Ho}}\frac{\partial \Theta}{\partial \tau} + \frac{\partial \Psi}{\partial Y}\frac{\partial \Theta}{\partial X} - \frac{\partial \Psi}{\partial X}\frac{\partial \Theta}{\partial Y} = \frac{1}{\text{Pr}\sqrt{\text{Gr}}}\Delta\Theta\,; \tag{3}$$

for the elements of the solid material

$$\frac{1}{\text{Fo}_i}\frac{\partial \Theta_i}{\partial \tau} = \Delta\Theta_i\,, \quad i = \overline{1, 3}\,. \tag{4}$$

We will write the initial and boundary conditions for the formulated problem (1)–(4):

the initial condition

$$\Psi\,(X, Y, 0) = 0\,, \quad \Omega\,(X, Y, 0) = 0\,, \quad \Theta\,(X, Y, 0) = 0\,,$$

except for the heat release source over which $\Theta = 1$ in the course of the entire process;

the boundary conditions:

at the boundary $X = 0$ that separates the external environment and the computational domain the boundary conditions that account for heat transfer by convection and radiation are written:

TABLE 1. Average Nusselt Numbers Depending on the Grashof Number and on the Value of the Relative Heat Conduction Coefficient

Gr	λ_s/λ_f	Results obtained	Literature data [4]	Literature data [12]
	1	0.872	0.877	0.87
10^3	5	1.023	—	1.02
	10	1.046	—	1.04
	1	2.116	2.082	2.08
10^5	5	3.421	—	3.42
	10	3.781	—	3.72
	1	3.002	2.843	2.87
10^6	5	6.306	—	5.89
	10	6.935	—	6.81

$$\frac{\partial \Theta_i (X, Y, \tau)}{\partial X} = \mathrm{Bi}_i \Theta_i (X, Y, \tau) + \mathrm{Bi}_i \frac{T_0 - T_e}{T_{h.s} - T_0} + Q_i ,$$

$$Q_i = \mathrm{N}_i \left[\left(\Theta_i (X, Y, \tau) + \frac{T_0}{T_{h.s} - T_0} \right)^4 - \left(\frac{T_e}{T_{h.s} - T_0} \right)^4 \right], \quad i = 1, 3 \quad \text{(Fig. 1)};$$

at the remaining outer boundaries the conditions of thermal insulation are prescribed:

$$\frac{\partial \Theta_i (X, Y, \tau)}{\partial X^k} = 0 , \quad X^1 \equiv X , \quad X^2 \equiv Y , \quad i = \overline{1, 3} ;$$

over all the portions of the solution domain, where conjunction of materials with different thermophysical parameters occurs, the conditions of the 4th kind are met:

$$\Theta_i = \Theta_j , \quad \frac{\partial \Theta_i}{\partial X^k} = \lambda_{j,i} \frac{\partial \Theta_j}{\partial X^k} , \quad i, j = \overline{1, 4} , \quad i \neq j , \quad k = 1, 2 ;$$

at the inner boundary between the solid material and gas, parallel to the $0X$ axis:

$$\Psi = 0 , \quad \frac{\partial \Psi}{\partial Y} = 0 , \quad \Theta_3 = \Theta_4 , \quad \frac{\partial \Theta_3}{\partial Y} = \lambda_{4,3} \frac{\partial \Theta_4}{\partial Y} ;$$

at the inner boundaries between the solid material and gas, parallel to the $0Y$ axis:

$$\Psi = 0 , \quad \frac{\partial \Psi}{\partial X} = 0 , \quad \Theta_1 = \Theta_4 , \quad \frac{\partial \Theta_1}{\partial X} = \lambda_{4,1} \frac{\partial \Theta_4}{\partial X} .$$

Solution of the Problem. The problem (1)–(4) with the corresponding boundary and initial conditions is solved by the method of finite differences [5, 6]. Equations (1)–(4) were solved consecutively; each time step started from calculation of the temperature field in both the gas cavity and the elements of the solid material (Eqs. (3) and (4)) and thereafter the Poisson equation for the stream function (2) was solved. Subsequently the boundary conditions for the vorticity vector were determined using the Woods formula, and Eq. (1) was solved.

In order to carry out the numerical solution of Eq. (1) a difference scheme of alternating directions was used. Approximation of the convective terms was considered averaged over U and $|U|$ (V and $|V|$) so that the scheme could be independent of the velocity sign. An implicit difference scheme was used. The evolution term was a one-sided difference in time and had the first order of accuracy relative to the step in time. All of the derivatives with respect to the space coordinates were approximated with the second order of accuracy relative to the step in space.

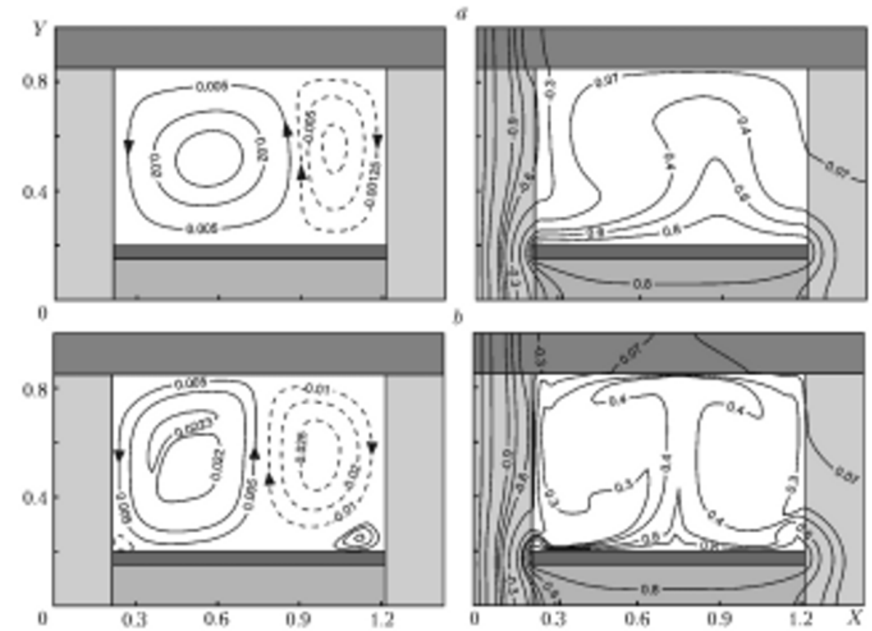

Fig. 2. Typical streamlines Ψ and temperature fields Θ at $\tau = 5.3{\cdot}10^4$: a) Gr = 5; b) 10^8.

The solution of Eq. (2) was found by the time-dependent method. The condition of attainment of the "stationary" conditions had the form

$$\max_{l,m} \left| \Psi_{l,m}^{n+1} - \Psi_{l,m}^{n} \right| < \varepsilon_{\text{p}} \, .$$

Equations (3) and (4) were solved using the A. A. Samarskii locally one-dimensional scheme, and to resolve the nonlinear boundary condition of the 3rd kind the method of simple iteration was used. The method of solution was tested on a model problem. A plane laminar convective flow of a viscous heat-conducting liquid in a closed square region as well as heat transfer in one of the walls having finite dimensions and the heat conduction coefficient different from 0 and ∞ were considered. The vertical walls were kept at different constant temperatures. The results under the following values of the determining parameters were compared: Pr = 0.71 and Ho = 1. The solutions were obtained up to Gr = 10^6. As the criterion of the comparison of solutions [4, 12] and that obtained in the present work the average Nusselt number was used at the boundary between the solid wall and the gas (see Table 1). The values of Nu presented in the table clearly show that the method used leads to fairly good agreement with the works of other researchers.

Results of Calculations. Numerical investigations of the boundary-value problem (1)–(4) with the corresponding initial and boundary conditions were carried out at the following values of dimensionless numbers: Ho = 1, Gr = 10^5–10^8, and Pr = 0.71. The dimensionless determining temperatures had the following values: $\Theta_{\text{e}} = -2$, $\Theta_{\text{h.s}} = 1$, and $\Theta_0 = 0$.

Figure 2 presents the streamlines and temperature fields that correspond to the regimes of convective heat transfer at Gr = 10^5 and 10^8. The arrows at the lines indicate the direction of gas motion. At Gr = 10^5 and 10^8 two convective cells are formed in the gas cavity; they are distinguished by the scales of the region occupied and by the direction of flow.

At Gr = 10^5 (Fig. 2a) the counterclockwise motion occupies a larger region as compared to the clockwise flow. The reason for such a distribution of the streamlines is the nonlinear influence of the surrounding medium which leads to the propagation of the lowered temperature from the boundary $X = 0$ into the depth of the computational domain, which is evident from the distribution of isotherms. The temperature field is rather nonuniform due to the dynamics of conductive heat transfer in the left element of the solid material, as well as to the mutual influence of

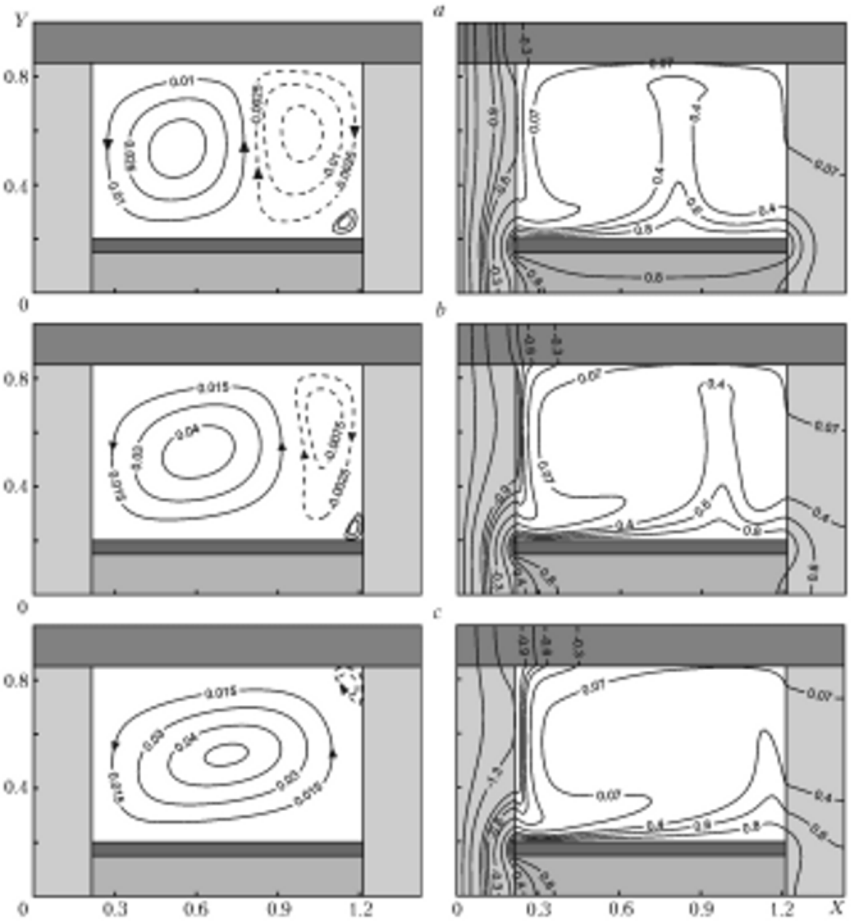

Fig. 3. Typical streamlines Ψ and temperature fields Θ at Gr = 10^6: a) τ = $5.3 \cdot 10^4$; b) $10.6 \cdot 10^4$; c) $15.9 \cdot 10^4$.

convective heat transfer in the gas cavity and conductive heat transfer in the solid wall. For these reasons the "coordinate maximum" of the isotherms shifts to the right wall.

At Gr = 10^8 (Fig. 2b) the scales of circulation flows and the structure of the counterclockwise motion change, and the velocity of the clockwise motion increases as compared to the regime with Gr = 10^5. At Gr = 10^8 secondary vortices are formed in the corner zones of the solution domain, which is explained by the increased velocities of motion. The temperature distribution changes substantially — a clear temperature "mushroom" appears, which corresponds to a dimensionless temperature equal to 0.4. Also, the conductive heat transfer in the upper element of the solid material is intensified due to the effect of convective flow in the gas cavity (the isotherm corresponding to a dimensionless temperature equal to 0.07 moves deeper into the upper element of the solid material).

An analysis of the effect of the nonstationarity factor on the distribution of thermal and hydrodynamic characteristics has been carried out. Figure 3 presents the streamlines and temperature fields that correspond to the regime of flow with Gr = 10^6 at different time instants.

At τ = $5.3 \cdot 10^4$ (Fig. 3a) two convective cells having different scales and different velocities of gas motion are formed in the gas cavity. In the right corner zone of the bottom a secondary flow is formed. In the gas cavity a definite temperature field is also formed which begins to rearrange due to the effect of the dynamics of conductive heat transfer in the left element of the solid material due to the effect of the surrounding medium.

The increase in time up to τ = $10.6 \cdot 10^4$ (Fig. 3b) leads to a change in both the flow pattern and in the temperature field. The vortex that corresponds to the counterclockwise motion increases in size and deforms the circulation flow located near the right element of the solid material. In this case, the increase in velocity of the counterclockwise gas motion is noticeable. The secondary flow near the bottom decreases in dimensions and becomes more "com-

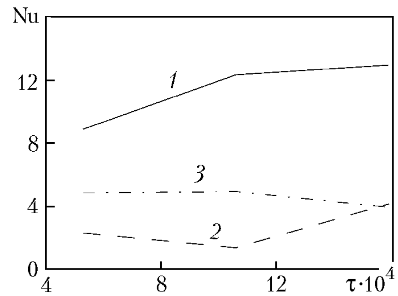

Fig. 4. Average Nusselt number vs. time at Gr = $\cdot 10^6$: 1) Nu_1; 2) Nu_2; 3) Nu_3.

pressed" to the right wall. The temperature distribution shows once again that natural convection is characterized by the mutual effect of the velocity and temperature fields. A more substantial motion of the isotherms of lowered temperature deeper into the solution domain from the boundary $X = 0$ occurs; also a "cold wave" in the zone $0.21 < X < 0.6$ and $0.2 < Y < 0.4$ is noticeable.

With further increase in τ (Fig. 3c) the size of the main vortex increases appreciably, which leads to the transition of the circulation flow, which earlier was located near the right wall, into the class of secondary flows in the corner zone with $1.1 < X < 1.21$ and $0.73 < Y < 0.85$. The temperature field also changes substantially — the temperature in the region of the upper element of the solid wall drops (the isotherm corresponding to the dimensionless temperature 0.4 is compressed to the source of heat release, and its "coordinate maximum" tends to the right element of the solid material).

We also carried out an analysis of the influence of the nonstationary factor on the value of the average Nusselt number of three boundaries of the gas cavity and elements of the solid material:

$$Nu_1 = \frac{1}{0.65}\int_{0.2}^{0.85}\left|\frac{\partial\Theta}{\partial X}\right|_{X=0.21} dY\,, \quad Nu_2 = \frac{1}{0.65}\int_{0.2}^{0.85}\left|\frac{\partial\Theta}{\partial X}\right|_{X=1.21} dY\,, \quad Nu_3 = \int_{0.21}^{1.21}\left|\frac{\partial\Theta}{\partial X}\right|_{Y=0.85} dX\,.$$

Figure 4 demonstrates the average Nusselt number on three walls vs. time. It is seen that the values of the dimensionless heat transfer coefficient on three "gas cavity–element of the construction" phase interfaces differ substantially.

The increase in Nu_1 with τ is explained by the increase in the temperature gradient due to the movement of the isotherms of the lowered temperature from the boundary $X = 0$. In this case Nu_2 behaves nonmonotonically, which is confirmed by the dynamics of the temperature field (see Fig. 3). At $\tau = 10.6\cdot 10^4$ the value of Nu_2 decreases in comparison with its value at $\tau = 5.3\cdot 10^4$. From the distribution of the isotherms in the figure it is seen that the temperature "coordinate maximum" approaches the right wall, and, correspondingly, the temperature in this zone starts to increase, which is reflected in the behavior of Nu_2. When the value $\tau = 15.9\cdot 10^4$ is attained, Nu_2 starts to increase again due to the attainment of the temperature "coordinate maximum" of the right wall. In this case, the temperature profile corresponding, e.g., to the isotherm of the dimensionless temperature 0.4, has an inflexion point on the wall, which leads to an increase in the temperature gradient.

The dependence of Nu_3 on time is also nonmonotonic. The reason for such a distribution is the substantially nonstationary character of the process investigated.

The results obtained made it possible to derive correlations for average Nusselt numbers depending on the Grashof number at fairly large values of τ, $\tau = 5.3\cdot 10^4$ in the range of change in the Grashof number $10^6 \le Gr \le 10^8$:

$$Nu_1 = 0.284 Gr^{0.247}\,; \quad Nu_2 = 0.138 Gr^{0.195}\,; \quad Nu_3 = 0.118 Gr^{0.266}\,.$$

These expressions for the dimensionless heat transfer coefficient show that even at relatively simple (laminar) regimes of flow the conditions of heat exchange between the cooling gas and the surfaces of heat release depend substantial on the orientation of the zone of intense heat release and of the phase interface between the considered system and the surrounding medium. The singled-out trends create certain prerequisities for selecting the geometric parameters and thermophysical characteristics of the materials used, as well as (which is most important) constructive solutions in design development of the variants of small-size specimens of REF and E with intense heat release. These factor have a particular importance under conditions where the cooling of the heat releasing units or blocks in the regime of forced convection is impossible, e.g., because of rigid limitations due to dustiness, humidity, electrostatic electricity, etc.

Conclusions. The regimes of conjugate thermogravitational convection of gases in a closed rectangular cavity were investigated numerically in the range of change of the determining number $10^5 \le \mathrm{Gr} \le 10^8$. The specific features of the distributions of the streamlines and temperature corresponding to different regimes of flow have been distinguished. The influence of the nonstationary factor, which is conditioned not only by the possible time-variable effect of the surrounding medium but also by the thermal inertia of the solid material elements, is shown. Correlations for determining the average Nusselt number on the boundaries of the gas cavity and solid wall in the range of the Grashof number investigated have been obtained. These dependences can be used to determine the generalized coefficient of heat transfer of typical electroradioelements under the conditions of operation of REE. The latter conclusion to a certain extent characterizes the multifactor nature of the relations obtained, since here not only processes of convection in the "working" cavity are taken into account but also heat transfer in the walls of a device and also the influence of the surrounding medium.

The work was carried out with financial support from the Russian Foundation for Basic Research and administration of the Tomsk region (No. 05-02-98006).

NOTATION

a, thermal diffusivity, m^2/sec; $\mathrm{Bi}_i = \alpha L/\lambda_i$, Biot number corresponding to the ith material; $\mathrm{Fo}_i = a_i t_0/L^2$, Fourier number corresponding to the ith material; $\mathrm{Gr} = \beta g_y L^3 (T_{\mathrm{h.s}} - T_0)/\nu^2$, Grashof number; g_y, component of the gravity force in the projection onto the y axis ($g_x = 0$), m/sec^2; $\mathrm{Ho} = V_0 t_0/L$, homochronicity number; L, size of the gas cavity of the solution domain over the x axis, m; L_x, size of the solution domain over the x axis, m; L_y, size of the solution domain over the y axis, m; $\mathrm{N}_i = \varepsilon\sigma L(T_{\mathrm{h.s}} - T_0)^3/\lambda_i$, Stark number corresponding to the ith material; Nu_1, value of the average Nusselt number on the boundary $X = 0.21$, $0.2 < Y < 0.85$; Nu_2, value of the average Nusselt number on the boundary $X = 1.21$, $0.2 < Y < 0.85$; Nu_3, value of the average Nusselt number on the boundary $Y = 0.85$, $0.21 < Y < 1.21$; $\mathrm{Pr} = \nu/a$, Prandtl number; Q_i, dimensionless heat flux that determines the role of conduction and radiation on the boundary of the ith material; T, temperature, K; T_{e}, external temperature, K; T_0, initial temperature of the solution domain, K; $T_{\mathrm{h.s}}$, temperature of the heat source, K; t, time, sec; t_0, time scale, sec; U, V, dimensionless velocity components corresponding to u and v; $V_0 = \sqrt{g_y \beta (T_{\mathrm{h.s}} - T_0) L}$, velocity scale (velocity of convection), m/sec; u, v, velocity components in the projection onto the x and y axis, respectively, m/sec; X and Y, dimensionless coordinates corresponding to x and y; X^k, kth ort of the coordinate system; x and y, Cartesian coordinates; α, heat transfer coefficient, W/(m^2·K); β, temperature coefficient of volumetric expansion, K^{-1}; Δ, Laplace operator; ε, reduced emissivity; ε_{p}, accuracy of calculations; Θ, dimensionless temperature; Θ_0, initial dimensionless temperature of the solution domain; Θ_{e}, dimensionless temperature of the surrounding environment; $\Theta_{\mathrm{h.s}}$, dimensionless temperature on the heat source; Θ_i, dimensionless temperature of the ith material; λ_i, heat conduction coefficient of the ith material, W/(m·K); $\lambda_{ij} = \lambda_i/\lambda_j$, relative heat conduction coefficient; ν, coefficient of kinematic viscosity, m^2/sec; σ, Stefan–Boltzmann constant, W/(m^2·K^4); τ, dimensionless time; Ψ, dimensionless stream function corresponding to ψ; ψ, stream function; $u = \partial\psi/\partial y$, $v = -\partial\psi/\partial x$, m^2/sec; $\psi_0 = V_0 L$, scale of the stream function, m^2/sec; Ω, dimensionless vorticity of velocity corresponding to ω; ω, velocity vorticity, $\omega = 0.5\,(\partial v/\partial x - \partial u/\partial y)$, 1/sec; $\omega_0 = V_0/L$, scale of velocity vorticity, 1/sec. Subscripts: 0, initial time instant; e, environment; f, fluid; h.s, heat source; i, j, number of the material; k, ordinal number of the curl of the coordinate system; l, m, coordinates of the grid node; n, number of iteration; p, precision; s, element of the solid material.

REFERENCES

1. B. Abourida and M. Hasnaoui, Numerical study of partitions effect on multiplicity of solutions in an infinite channel periodically heated from below, *Energy Conversion and Management*, **46**, 2697–2717 (2005).
2. G. N. Dul'nev, *Methods of Calculation of the Thermal Regime of Instrumentation* [in Russian], Radio i Svyaz', Moscow (1990).

3. A. V. Luikov, A. A. Aleksashenko, and V. A. Aleksashenko, *Conjugate Problems of Convective Heat Transfer* [in Russian], Nauka i Tekhnika, Minsk (1971).
4. A. Liaqat and A. C. Baytas, Conjugate natural convection in a square enclosure containing volumetric sources, *Int. J. Heat Mass Transfer*, **44**, 3273–3280 (2001).
5. G. V. Kuznetsov and M. A. Sheremet, Modeling of nonstationary heat transfer in a closed region with a local heat-release source, *Teplofiz. Aéromekh.*, **12**, No. 2, 305–314 (2005).
6. G. V. Kuznetsov and M. A. Sheremet, Conjugate heat transfer in a closed domain with a locally lumped heat-release source, *Inzh.-Fiz. Zh.*, **79**, No. 1, 56–63 (2006).
7. A. W. Goetling, *Rayleigh–Benard Convection. Structure and Dynamics* [Russian translation], Éditorial URSS, Moscow (1999).
8. Y. Jaluria, *Natural Convection. Heat and Mass Transfer* [Russian translation], Mir, Moscow (1983).
9. Yu. A. Sokovishin and O. G. Martynenko, *Introduction to the Theory of Free Convective Heat Transfer* [in Russian], Izd. LGU, Leningrad (1982).
10. B. Gebhart, Y. Jaluria, R. L. Mahajan, and B. Sammaki, *Buoyancy-Induced Flows and Transport* [Russian translation], Vol. 1, Mir, Moscow (1991).
11. A. V. Luikov, *Heat Conduction Theory* [in Russian], Vysshaya Shkola, Moscow (1967).
12. D. A. Kaminski and C. Prakash, Conjugate natural convection in a square enclosure: effect of conduction on one of the vertical walls, *Int. J. Heat Mass Transfer*, **29**, 1979–1988 (1986).